Fabrication of Hybrid Ladderlike Polysilsesquioxane-Grafted Multiwalled Carbon Nanotubes

Seung-Hwa Lee, Jung-Hyurk Lim, Kyung-Min Kim

Department of Polymer Science and Engineering, Chungju National University, Chungju, Chungbuk 380-702, Korea

Received 26 July 2010; accepted 30 July 2011
DOI 10.1002/app.35389
Published online 23 November 2011 in Wiley Online Library (wileyonlinelibrary.com).

ABSTRACT: Ladderlike polysilsesquioxanes (LPSs) containing chloromethylphenyl groups were synthesized from (*p*-chloromethyl)phenyltrimethoxysilane under basic conditions. Functionalized multiwalled carbon nanotubes (MWNT–COOH) were prepared by the acid treatment of pristine multiwalled carbon nanotubes (MWNTs). MWNT–COOH was reacted with LPS to prepare LPS-grafted MWNTs via ester linkages. The functionalization of MWNTs with LPS significantly altered the surface roughness of the MWNTs; there was a significant increase in the diameter of the MWNTs. The LPS-grafted MWNTs had a 10–20 nm thickness along the outer walls according to the functionalization of the MWNTs with LPS. An advantage of the hybrid LPS-grafted MWNTs was shown as improved thermal behavior. The composition, thermal properties, and surface morphology of the LPS-grafted MWNTs were studied by Fourier transform infrared spectroscopy, thermogravimetric analysis, energy-dispersive spectroscopy, scanning electron microscopy, atomic force microscopy, and transmission electron microscopy. © 2011 Wiley Periodicals, Inc. J Appl Polym Sci 124: 3792–3798, 2012

Key words: carbon nanotube; nanocomposites; TEM

INTRODUCTION

Organic polymers have good properties, including lightness, flexibility, and processability, even when they have a low heat-resistance and weak mechanical stiffness. On the other hand, inorganic materials are superior to organic polymers in their thermal and mechanical properties and transparency. Thus, many efforts have been made to create new hybrid materials with enhanced physical properties through the merits of each material by the combination of both an organic polymer and an inorganic ceramic.[1,2]

Polyhedral oligomeric silsesquioxanes (POSSs) are a well-defined cage cluster with an inorganic silica-like core (Si_8O_{12}) surrounded by eight organic functional groups. POSSs not only have unique hybrid chemical compositions with nanosized cage structures but also provide a variety of property enhancements, as observed in POSS copolymers and blends.

Ladderlike polysilsesquioxanes (LPSs) with an $(RSiO_{3/2})_n$ formula, where R is an organic substituent, have been used as useful molecular building blocks in the formation of organic–inorganic hybrid nanocomposites.[3–8] LPSs with various organic functional groups can react with organic monomers, oligomers, and polymers to give organic–inorganic hybrid materials.[9] It is expected that LPSs are useful for starting hybrid polymers for the synthesis of various hybrid materials because they have excellent thermal stability and fire resistance and good mechanical properties.[10–12] The diverse uses of LPSs included photopatternable films, polymer network liquid crystals, and nonlinear optical films.[13–15] The crosslinked nature and rigid structure of LPSs confer them a higher glass-transition temperature in addition to a higher thermal stability compared to POSSs.

Carbon nanotubes (CNTs), which have been spotlighted by many laboratories in various fields, are nanosized carbon materials with a thin and long tube shape of reciprocally coupled hexagons formed by six carbons. The structure of CNTs is an sp^2 combination structure in which one carbon atom combines with the next three carbon atoms, like in the case of graphite. CNTs fall into categories of single-walled nanotubes and multiwalled carbon nanotubes (MWNTs), depending on the number of layers of graphite.[16,17] As described previously, CNTs with such unique structures have a conductivity similar to that of copper, a thermal conductivity similar to that of diamond, and a characteristic stiffness superior to that of steel. CNTs show various chemical,

Correspondence to: K.-M. Kim (kmkim@chungju.ac.kr).

Contract grant sponsor: Basic Science Research Program through the National Research Foundation of Korea, funded by the Ministry of Education, Science and Technology; contract grant number: 2010-0016092.

Contract grant sponsor: Ministry of Education, Science, and Technology and National Research Foundation of Korea through the Human Resource Training Project for Regional Innovation.

mechanical, and electrical characteristics, depending on their length, diameter, and structure. Because of their potential applications, many researchers have studied various fields based on CNTs, including nanoelectronics, chemical sensors, nanoelectromechanical systems, and hydrogen storage materials.[18–20] Also, various polymer composites with CNTs have attracted considerable attention for the fabrication of new advanced materials with improved mechanical strength, unique multifunctional properties, and excellent processability.[21–26]

Polymer/CNT composites are easily fabricated by chemically functionalized CNTs with polymers via grafting-from or grafting-to techniques or by the blending of CNTs and polymers by melt processing.[27–29] We previously synthesized hybrid nanocomposites of polystyrene and MWNTs with well-defined polystyrene via multiple atom transfer radical polymerization approach[30] and fabricated nanocomposites of palladium nanoparticles having POSSs and MWNTs via ionic interactions.[31]

In this article, we report new hybrid LPS-grafted MWNTs with a double-chain linear network containing Si—O—Si units by the reaction of functionalized multiwalled carbon nanotubes (MWNT–COOH) and LPS. Such a rigid main-chain-structured material showed great merits for heating safety and a low dielectric constant. This report provides great interest in the semiconductor field by providing such characteristics.[32–34] The new hybrid LPS-grafted MWNTs had a 10–20 nm thickness along the outer walls of the MWNTs due to the introduction of LPSs to the surfaces of the MWNTs. The LPS-grafted MWNTs showed excellent thermal stability.

EXPERIMENTAL

Materials

Pristine MWNTs were obtained from Iljin Nanotech, Inc. (Seoul, Korea) (diameter = 10–20 nm, length = 10–50 μm, >90 vol % purity). (*p*-Chloromethyl)phenyltrimethoxysilane (CPTS; JSI Silicone) was dried with CaH_2 and purified by distillation before use. *N,N*-dimethylformamide (DMF) and toluene were distilled over sodium and calcium hydride, respectively. The other reagents were used as supplied without further purification.

Characterization

^{1}H-NMR spectra were obtained on a Bruker 400-MHz AVANCE 400FT NMR spectrometer (Seoul, Bruker Korea). Fourier transform infrared (FTIR) spectra were recorded on a Bio-Rad FTS-6000 spectrometer. The thermal behavior was examined with thermogravimetric analysis (TGA; TGA S-1000, SCINCO) under atmosphere. A Raman spectrophotometer (NRS-3200, Jasco) was used to confirm and characterize the LPS-grafted MWNTs. The morphologies and compositions of the LPS-grafted MWNTs were observed by atomic force microscopy (AFM; XE-1000, Park Systems), scanning electron microscopy (SEM; JSM-6700, JEOL), energy-dispersive spectroscopy, and energy-filtering transmission electron microscopy (EF-TEM; Libra 120, Zeiss). For EF-TEM observation, the LPS-grafted MWNTs were redissolved in DMF, and the solution was dropped onto a copper grid and then dried *in vacuo*. The molecular weight and polydispersity index of LPS were investigated by gel permeation chromatography with an Agilent Technologies 1200 series instrument. Polystyrene standards were used for calibration, and tetrahydrofuran (THF) was used as the eluent at a flow rate of 1.0 mL/min.

Acid treatment of the pristine MWNTs

Typically, 6.0 g of crude MWNTs, 50 mL of 60% HNO_3, and 150 mL of 98% H_2SO_4 were added to a 500-mL flask equipped with a condenser. The flask was then immersed in a sonication bath (40 kHz) for 90 min. The mixture was then stirred for 3 h under reflux (90°C). During this period, a dense brown gas was collected and was treated with an NaOH aqueous solution connected to the condenser by a plastic tube. After it was cooled to room temperature, the reaction mixture was diluted with 500 mL of deionized water and then vacuum-filtered through filter paper. The dispersion, filtering, and washing steps were repeated until the pH of the filtrate reached 7 (at least four cycles were required). The filtered solids were then washed with about 100 mL of acetone and THF five times to remove most of the water from the sample and dried *in vacuo* for 24 h at 60°C.

Synthesis of LPS

A 100-mL, round-bottom flask was charged with CPTS (2.46 g, 10.0 mmol), triethylamine (TEA; 0.10 g, 1.0 mmol), toluene (40 mL), and water (20 mL). Then, the solution was sealed with a rubber septum. The mixture was stirred at 60°C under a nitrogen atmosphere. The reaction was allowed to proceed for 24 h, and the reaction mixture was precipitated by dropwise addition of the solution into a large amount of methanol. The precipitates were redissolved in toluene and then precipitated into methanol. The white precipitates were collected by filtration and dried *in vacuo*. The product was analyzed by gel permeation chromatography (number-average molecular weight = 10,000 g/mol, polydispersity index = 2.89).

Yield: 1.02 g (68%). ^{1}H-NMR (400 MHz, $CDCl_3$, δ, ppm): 7.02 (br, aromatic H), 4.5 (br, CH_2Cl), 3.3 (br, $SiOCH_3$).

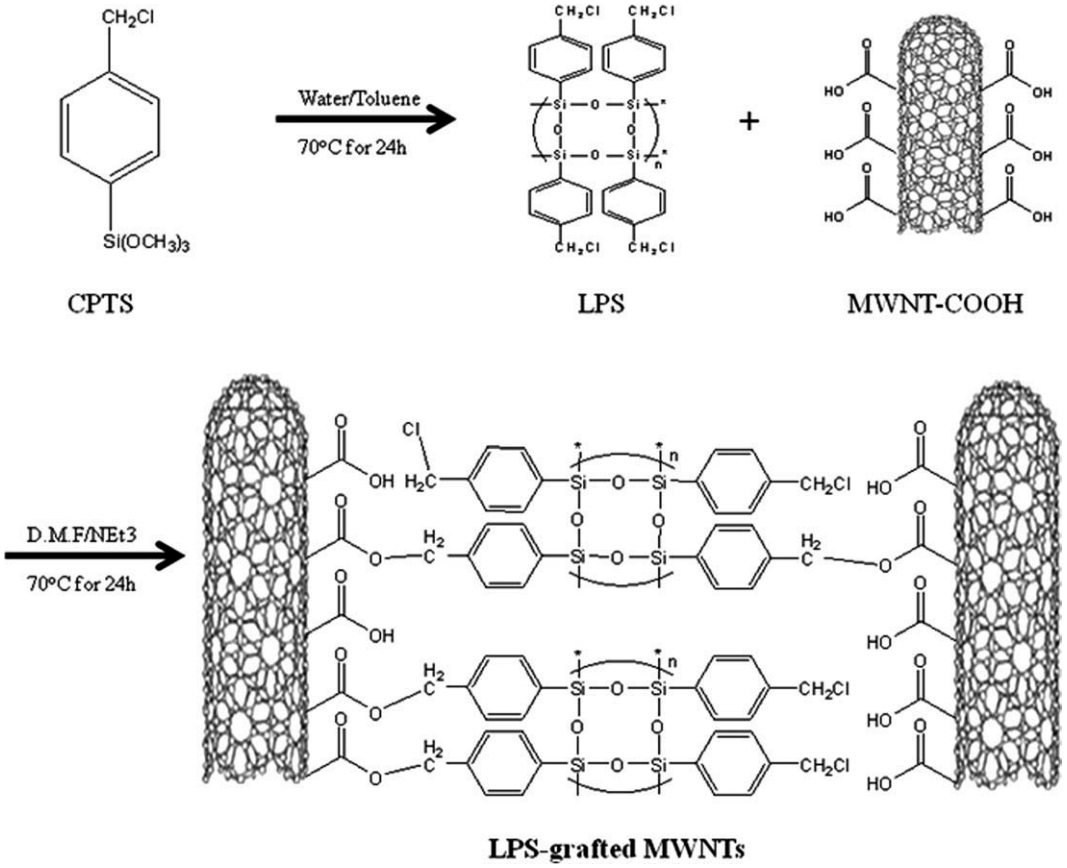

Scheme 1 Synthesis of LPS-grafted MWNTs.

Synthesis of the hybrid LPS-grafted MWNTs

MWNT–COOH (0.1 g) and DMF (30 mL) were introduced into a 100-mL flask, and the mixture was sonicated for 2 h. Then, LPS (1.0 g) and TEA (1.0 g, 10 mmol) were charged. After the mixture was stirred for 2 h at room temperature to form a black suspension, the glass was fitted with a condenser, and the mixture was stirred at 70°C under nitrogen for 72 h.

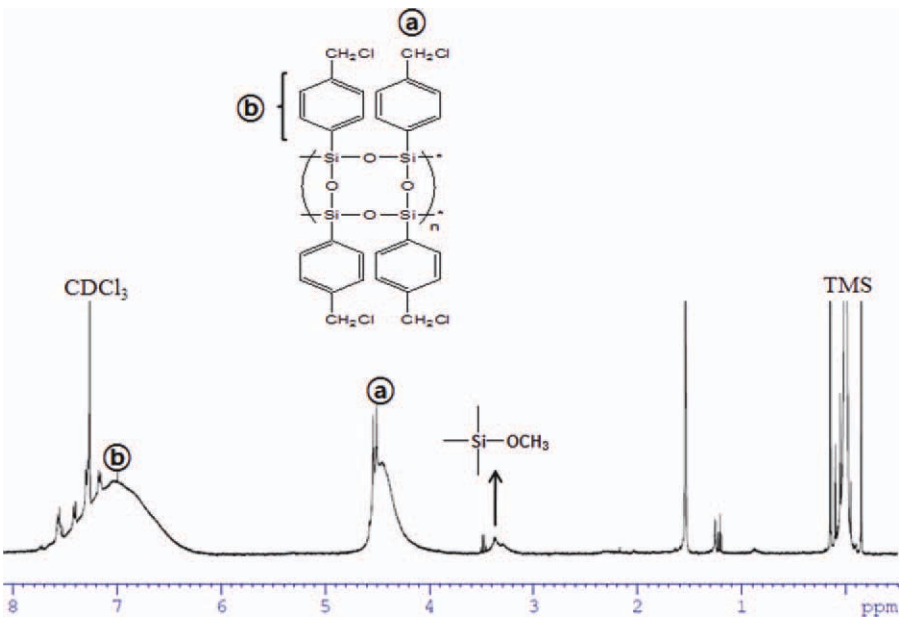

Figure 1 ^{1}H-NMR (400-MHz) spectra of LPSs in $CDCl_3$. [Color figure can be viewed in the online issue, which is available at wileyonlinelibrary.com.]

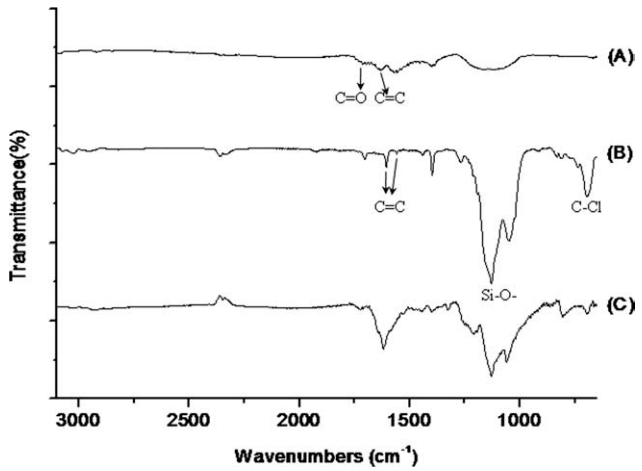

Figure 2 FTIR spectra of the (A) MWNT–COOH, (B) LPSs, and (C) LPS-grafted MWNTs with KBr.

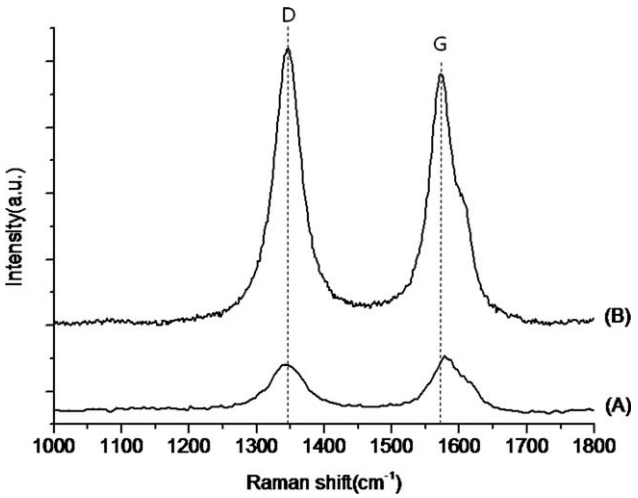

Figure 3 Raman spectra of the (A) pristine MWNTs and (B) LPS-grafted MWNTs.

After it was cooled to room temperature, the reaction mixture was diluted with 200 mL of DMF, and then, the mixture was sonicated for 40 min. The mixture was collected by filtration through a 200-nm-pore polycarbonate membrane with thorough washing with DMF, chloroform, and methanol, and then, the purified product was dried *in vacuo* overnight. The yield of the LPS-grafted MWNTs was 0.16 g (14%).

RESULTS AND DISCUSSION

It has already been reported that LPSs were easily obtained by the hydrolysis and condensation reaction of trimethoxysilane (TMS). According to those previous reports, the polycondensation of CPTS was carried out under the basic condition (Scheme 1).[34] The obtained LPSs were soluble in common organic solvents, such as dimethyl sulfoxide, DMF, THF, and $CHCl_3$. ^{1}H-NMR spectra showed the methyl protons of methoxysilyl moieties at 3.3 ppm, methylene protons of the chloromethyl moieties at 4.5 ppm, and aromatic protons at 7.02 ppm, as shown in Figure 1. The solubility of the LPS-grafted MWNTs was checked in various solvents. The LPS-grafted MWNTs were well dispersed in various solvents, including THF, DMF, and acetone. From these ^{1}H-NMR spectral data and the solubility of LPS, the polycondensation of CPTS with TEA as a catalyst mainly led to the formation of LPSs containing chloromethylphenyl groups in the side chains.

Figure 2 shows the FTIR spectra of the MWNT–COOH, LPSs, and LPS-grafted MWNTs. The spectra of the MWNT–COOH showed a C=C stretching peak at 1632 cm^{-1} and a C=O stretching peak at 1714 cm^{-1}, as shown Figure 2(A). In Figure 2(B), the characteristic absorption peaks of the LPSs showed C=C stretching peak of the aromatic moieties at 1504 and 1604 cm^{-1}, a Si—O—Si stretching peak at 1128 cm^{-1}, and a C—Cl stretching peak of chloromethyl groups at 696 cm^{-1}. After the surface modification of the MWNTs with LPSs, a new absorption

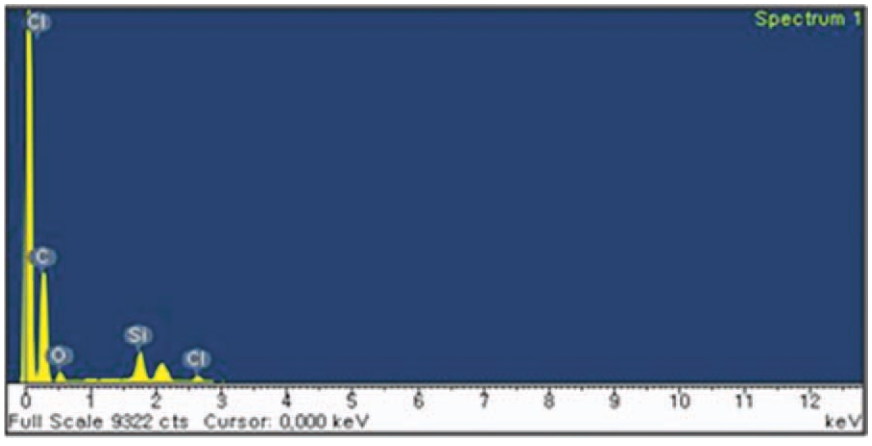

Figure 4 EDX spectra of the LPS-grafted MWNTs on carbon tape. [Color figure can be viewed in the online issue, which is available at wileyonlinelibrary.com.]

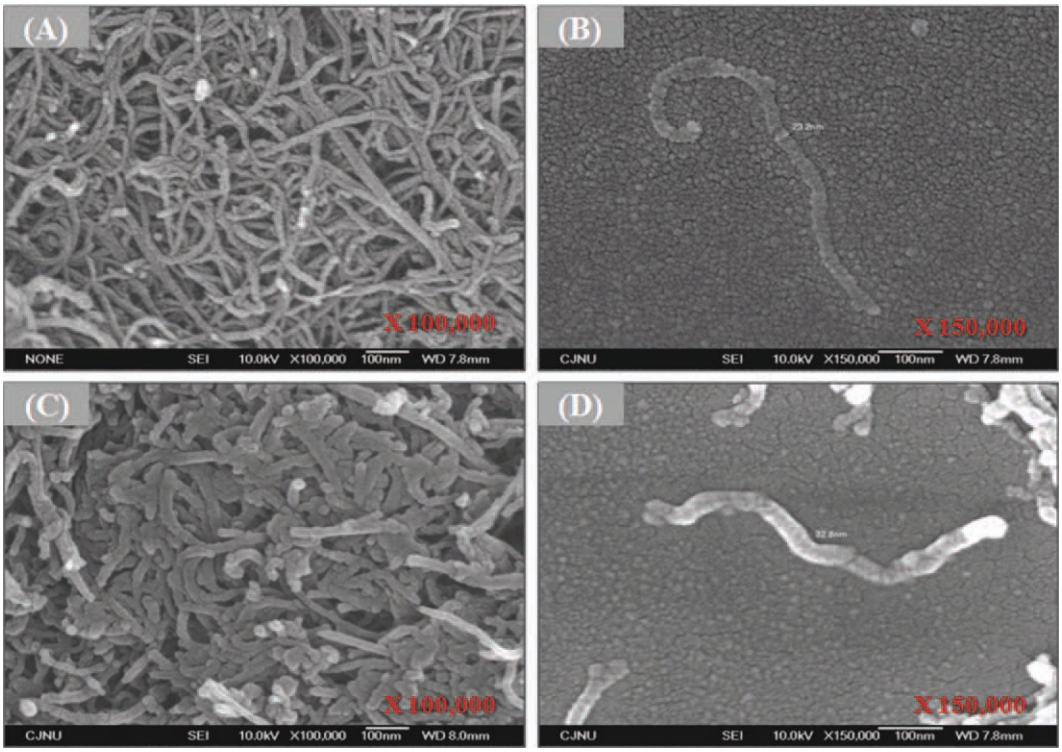

Figure 5 SEM images of (A) the pristine MWNTs, (B) a single pristine MWNT, (C) the LPS-grafted MWNTs, and (D) a single LPS-grafted MWNT on Si wafers. [Color figure can be viewed in the online issue, which is available at wileyonlinelibrary.com.]

peak for the aromatic ring in the region 1600–1440 cm^{-1} was observed as a result of the grafted LPSs onto the surfaces of the MWNTs. As shown in Figure 2(C), for the LPS-grafted MWNTs, two new peaks at 1128 and 696 cm^{-1} appeared; these were characteristic of LPSs and were not seen in the spectrum of MWNT–COOH.

Raman spectroscopy provided qualitative information about the LPS-grafted MWNTs. The Raman spectra of the pristine MWNTs and LPS-grafted MWNTs displayed two obvious peaks, as shown in Figure 3. This showed the characteristic G-mode, or the tangential mode peaks at 1580 cm^{-1}, and a disorder transition (D-band) peaks at 1345 cm^{-1} for the pristine and LPS-grafted MWNTs, respectively. In general, the intensity of the D band is used to probe the degree of modification. Figure 3(B) shows that the intensity enhancement of the D band in the LPS-grafted MWNTs proved the covalent bonding of LPSs onto the MWNTs. The ratio of the intensity of the D band to the ordered transition (G band), which indicated the generation of surface defects due to modification, increased from 0.98 (pristine MWNTs) to 1.03 (LPS-grafted MWNTs).

The composition of the LPS-grafted MWNTs was further confirmed by X-ray energy-dispersive

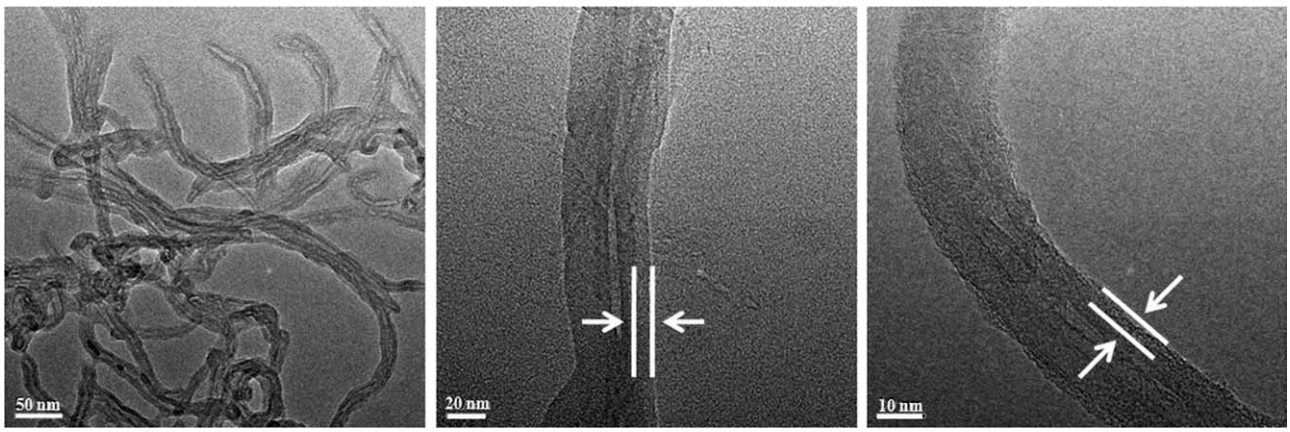

Figure 6 TEM images of the LPS-grafted MWNTs.

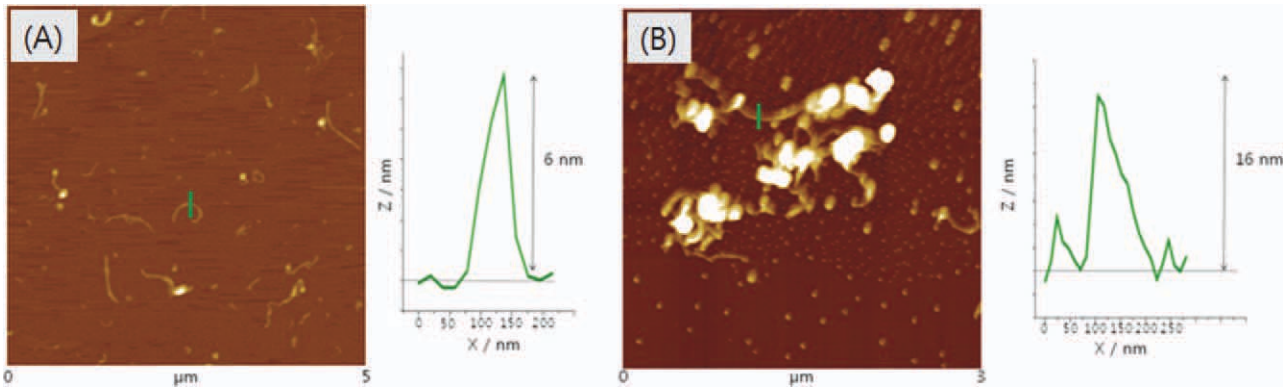

Figure 7 AFM images of the (A) MWNT–COOH and (B) LPS-grafted MWNTs. [Color figure can be viewed in the online issue, which is available at wileyonlinelibrary.com.]

spectroscopy analysis. Figure 4 shows a silicon peak at 1.74 keV, a carbon peak at 0.28 keV, an oxygen peak at 0.52 keV, and a chlorine peak at 2.62 and 0.2 keV in the LPS-grafted MWNTs. This result suggested that MWNT–COOH was functionalized with LPSs via ester linkages. That is, the LPSs were deposited well on the surfaces of the MWNT–COOH. However, the residue of chlorine in the LPS-grafted MWNTs was ascribed to the incomplete reaction between the chloromethyl groups of the LPSs and MWNT–COOH.

All of the aforementioned characterizations effectively demonstrated that well-defined LPSs were covalently grafted onto the MWNTs with a high loading efficiency. The measurement of SEM microscopy provided further direct evidence for the production of LPS-grafted MWNTs. SEM images of the pristine MWNTs and LPS-grafted MWNTs are shown in Figure 5. Figure 5(A,B) presents typical SEM images of the pristine MWNTs and shows a very clean surface for all of the MWNTs and a single pristine MWNT with a diameter of about 23 nm, respectively. However, the functionalization of MWNTs with LPSs significantly altered the surface roughness of the pristine MWNTs; there was a significant increase in the diameter of the MWNTs, as shown in Figure 5(C). It was clearly seen that a single LPS-grafted MWNT had a diameter of about 33 nm, as shown in Figure 5(D). This meant that a diameter with a 10-nm difference between the pristine MWNTs and the LPS-grafted MWNTs was derived from the attachment of LPSs onto the MWNTs.

Direct structural characterization of individual LPS-grafted MWNTs was realized by field emission transmission electron microscopy (FE-TEM) and AFM. The LPS-grafted MWNT images in FE-TEM and AFM are presented in Figures 6 and 7, respectively. As shown by the transmission electron microscopy (TEM) images, the LPS-grafted MWNTs exhibited polymer layers, including LPSs with a thickness around 10–20 nm along the outer walls of the MWNTs. In addition, the AFM images showed that the LPS-grafted MWNTs were 10 nm thicker than MWNT–COOH, as shown in Figure 7. The result is closely consistent with that of the SEM images mentioned previously. These results confirm that LPSs were deposited well onto the surface of the MWNTs by the reaction of LPSs and MWNT–COOH via ester linkages.

TGA was conducted to confirm the thermal stability of the LPS-grafted MWNTs. The residual content of MWNT–COOH was 2%, as shown in Figure 8(A). Figure 8(B) shows the residual content of LPS (ca. 33%). From this result, it is known that LPS contained silicon (ca. 33%) and organic functional groups (ca. 67%). Figure 8(A,C) shows that the difference from the residual content between MWNT–COOH and the LPS-grafted MWNTs was attributed to the loading of LPSs on the surfaces of MWNT–COOH by chemical reaction. In other words, the weight of the residue obtained from the LPS-grafted MWNTs (ca. 6%) was larger than that obtained from the MWNT–COOH (ca. 2%). This result suggests

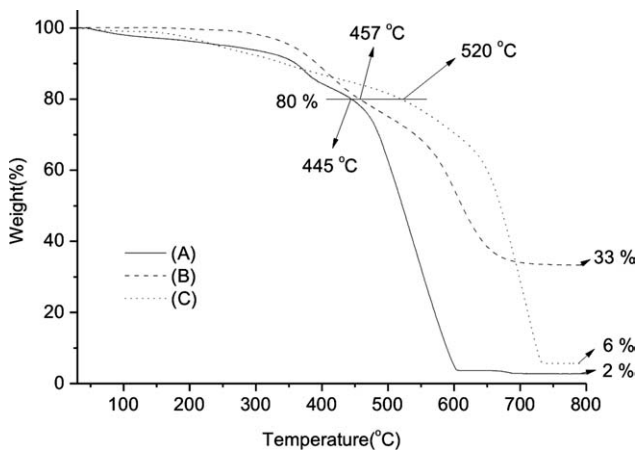

Figure 8 TGA curves of (A) MWNT–COOH, (B) LPSs, and (C) LPS-grafted MWNTs.

that the LPSs were deposited well on the MWNT–COOH. Furthermore, the thermal stability of the LPS-grafted MWNTs (520°C) at a 20% decomposition temperature was much higher than that of the MWNT–COOH (445°C) and LPS (457°C).

CONCLUSIONS

In summary, new hybrid LPS-grafted MWNTs were fabricated by the reaction of chloromethyl groups of LPSs and carboxylic acid groups of MWNT–COOH. ^{1}H-NMR, FTIR, and Raman analysis indicated that LPSs and LPS-grafted MWNTs were successfully prepared. As shown by SEM, TEM, and AFM images, the LPS-grafted MWNTs significantly altered the surface roughness of the MWNTs and caused a significant increase in the diameter of the MWNTs. That is, the LPS-grafted-MWNTs exhibited LPS layers with a thickness of 10–20 nm along the outer walls of the MWNTs. Furthermore, the TGA graph of the LPS-grafted MWNTs was totally shifted to the right compared to those of the MWNT–COOH and LPSs because of the increase in the thermal stability.

References

1. Wang, L. F.; Ji, Q.; Glass, T. E.; Ward, T. C.; McGrath, J. E.; Muggli, M.; Burns, G.; Sorathia, U. Polymer 2000, 41, 5083.
2. Kim, K. M.; Adachi, K.; Chujo, Y. Polymer 2002, 43, 1171.
3. Lichtenhan, J. D.; Otonari, Y. A.; Carr, M. J. Macromolecules 1995, 28, 8435.
4. Sellinger, A.; Laine, R. M. Macromolecules 1996, 29, 2327.
5. Sellinger, A.; Laine, R. M. Chem Mater 1996, 8, 1592.
6. Haddad, T. S.; Lichtenhan, J. D. Macromolecules 1996, 29, 7302.
7. Tsuchida, A.; Bolln, C.; Sernetz, F. G.; Frey, H.; Muelhaupt, R. Macromolecules 1997, 30, 2818.
8. Hedrick, J. L.; Hawker, C. J.; Miller, R. D.; Twieg, R.; Srinivasan, S. A.; Trollsas, M. Macromolecules 1997, 30, 7607.
9. Takahasi, T.; Katoh, T.; Sakuma, T.; Someya, Y.; Shibata, M. Polym Compos 2009, 30, 591.
10. Chiang, C. L.; Ma, C. C. M. J Polym Sci Part A: Polym Chem 2003, 41, 1371.
11. Krishnan, P. S. G.; He, C.; Shang, C. T. S. J Polym Sci Part A: Polym Chem 2004, 42, 4036.
12. Xie, P.; Zhang, R. Polym Adv Technol 1997, 8, 649.
13. Xie, P.; Sun, L. M.; Dai, D. R.; Liu, D. S.; Li, Z.; Zhang, R. B. Mol Cryst Liq Cryst 1995, 269, 75.
14. Xie, P.; Li, Z.; Zhang, R. B. Polym Bull 1995, 2, 65.
15. Xie, P.; Guo, J. S.; Dai, D. R.; Jin, S. Z.; Liu, D. S.; Li, Z.; Zhang, R. B. Polym Adv Technol 1996, 7, 98.
16. Nguyen, C. V.; Carter, K. R.; Hawker, C. J.; Hedrick, J. L.; Jaffe, R. L.; Miller, R. D.; Remenar, J. F.; Rhee, H. W.; Rice, P. M.; Toney, M. F.; Trollsas, M.; Yoon, D. Y. Chem Mater 1999, 11, 3080.
17. Ajayan, P. M. Chem Rev 1999, 99, 1787.
18. Popov, V. N. Mater Sci Eng Rev 2004, 43, 61.
19. Talapatra, S.; Kar, S.; Pal, S. K.; Vajtai, R.; Ci, L.; Victor, P.; Shaijumon, M. M.; Kaur, S.; Nalamasu, O.; Ajayan, P. M. Nat Nanotechnol 2006, 1, 112.
20. Nikitin, A.; Ogasawara, H.; Mann, D.; Denecke, R.; Zhang, Z.; Dai, H.; Cho, K.; Nilsson, A. Phys Rev Lett 2005, 95, 225507.
21. Coleman, J. N.; Khan, U.; Blau, W. J.; Gun'ko, Y. K. Carbon 2006, 44, 1624.
22. Moniruzzaman, M.; Winey, K. I. Macromolecules 2006, 39, 5194.
23. Qin, S.; Qin, D.; Ford, W. T.; Resasco, D. E.; Herrera, J. E. Macromolecules 2004, 37, 752.
24. Bose, S.; Khare, R. A.; Moldenaers, P. Polymer 2010, 51, 975.
25. Byrne, M. T.; Gun'ko, Y. K. Adv Mater 2010, 22, 1672.
26. Bauhofer, W.; Kovacs, J. Z. Compos Sci Technol 2009, 69, 1486.
27. Lopez Manchado, M. A.; Valentini, L.; Biagiotti, J.;Kenny J. M. Carbon 2005, 43, 1499.
28. Kim, K. H.; Jo, W. H. Carbon 2009, 47, 1126.
29. Wang, M.; Pramoda, K. P.; Goh, S. H. Polymer 2005, 46, 11510.
30. Jeon, J. H.; Lim, J. H.; Kim, K. M. Polymer 2009, 50, 4488.
31. Jeon, J. H.; Lim, J. H.; Kim, K. M. Macromol Res 2009, 17, 988.
32. Brown, J. F.; Vogt, L. H.; Katchman, A.; Eustance, K. W.; Kiser, K. M.; Krantz, K. W. J Am Chem Soc 1960, 82, 6194.
33. Chen, G. X.; Shimizu, H. Polymer 2008, 49, 943.
34. Kudo, H.; Yamamoto, M.; Nishikubo, T.; Moriya, O. Macromolecules 2006, 39, 1759.